Ultrabroad-Band Raman Amplifiers Pumped and Gain-Equalized by Wavelength-Division-Multiplexed High-Power Laser Diodes

Shu Namiki and Yoshihiro Emori

Invited Paper

***Abstract*—This paper reviews recent progress in broad-band Raman amplifiers for wavelength-division-multiplexed (WDM) applications. After the fundamentals of Raman amplifiers are discussed in contrast to erbium-doped fiber amplifiers, a new technique called "WDM pumping" is introduced to obtain ultra-broad and flat gain in Raman amplifiers only using WDM diode pumps. The design issues of this technique are then developed to realize outstanding performances such as 100 nm of flat gain bandwidth, 0.1 dB flatness over 80 nm, and so forth.**

***Index Terms*—Optical fiber, pump lasers, Raman amplifier, Raman scattering, WDM.**

I. Introduction

THE DRAMATIC growth of the Internet has invited unprecedented rapid deployment of wavelength-division-multiplexed (WDM) transmission systems based on erbium-doped fiber amplifiers (EDFAs), which are a cutting-edge technology yet. The insatiable demand of Internet to high-capacity data transport has dragged many newly born inventions out of labs into real fields, most of which may be maturing in the course of field applications. As a result, WDM transmissions are now using up the entire gain band of EDFA, i.e., C- and L-bands [1], [2]. Also, the spectral efficiency of transmission capacity has been increased up to 0.4 b/s/Hz by adopting the so-called dispersion-managed solitons [3]. Even though the entire band of EDFA is fully utilized and very high spectral efficiency was obtained through soliton technologies, the demands from Internet still seem to keep on growing recklessly. In order to satisfy the demands, a breakthrough has been sought in a sense: the EDFA-based WDM transmission technology has been hitting the upper limit of transmission capacity.

EDFAs used in WDM transmission systems are so-called lumped amplifiers in which the gain is lumped at a point of the transmission line. On the other hand, distributed amplifiers, such as fiber Raman amplifiers, retain the optical signal level over a long distance along the transmission line. This distributed amplification, in principle, shows better system performances especially in terms of noise. Fig. 1 elucidates how distributed amplifiers are superior to lumped amplifiers. A focus of system design is to optimize the signal level diagram: there is an upper limit and a lower limit in terms of signal level. If the signal enters into the fiber span at a too high level, it suffers from fiber nonlinearity, while if it enters at a too low level, it receives high noise at the next amplifier. In the systems based on lumped amplifiers, it is more difficult to resolve this dilemma than in those based on distributed ones, as depicted in Fig. 1. Now that EDFA-based systems are facing against a wall that bars toward higher capacity, it is time to reconsider fiber Raman amplifiers which are in nature a distributed amplifier.

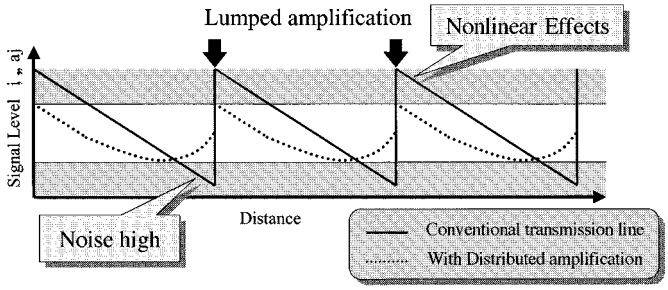

Fig. 1. Schematic diagram to compare a distributed amplifier and a lumped amplifier.

Raman amplification in optical fiber was first observed and measured by Stolen and Ippen [4]. Their measurement showed that the Stokes shift of Silica fiber is approximately 13.2 THz. Experiments on optical data transmission using Raman amplifiers were carried out by Aoki *et al.* [5]. And Mollenauer *et al.* utilized a fiber Raman amplifier to carry out optical soliton transmission [6]. Although it was even before EDFAs that Raman amplifiers were demonstrated in experiments using large-scale solid-state lasers, they were not actually deployed in the real field systems. Raman amplifiers could not have been deployed until very recently when high-power diode pump sources became commercially available [7], [8]. Meanwhile, EDFAs using diode pump lasers have been widely studied and actually deployed in the WDM systems [9], [10]. It is a coincidence that both EDFA and Raman amplifier are pumped at around 1480 nm for 1550-nm signal band. As pump laser

Manuscript received November 29, 2000; revised February 9, 2001.

The authors are with Fitel Photonics Lab, Furukawa Electric Co., Ltd., Ichihara, Chiba 290-8555, Japan (e-mail: snamiki@ch.furukawa.co.jp).

Publisher Item Identifier S 1077-260X(01)04465-3.

diodes became mature and powerful due to strong demand of high capacity [7], [8], [11], the feasibility of Raman amplifiers has increased accordingly. 14XX-nm pump laser diodes have achieved more than 300 mW at commercial level [12]. There has also been an alternative approach for achieving watt-class 1480-nm outputs based on the so-called cascaded Raman laser technology [13].

Despite the deployment of EDFA in the real-field applications, studies on Raman amplifiers have been continually conducted to suggest two critical merits of Raman amplifier: one is low noise and the other is arbitrary gain band. Hansen *et al.* showed that a 2.5-Gb/s system could be upgraded to 10 Gb/s by only adding Raman amplification [14]. Nissov *et al.* demonstrated a 7200-km WDM transmission using only Raman amplifiers. They also showed that the system based only on Raman amplifiers has superior noise performance to an EDFA based system [15]. Masuda *et al.* demonstrated that a Raman amplifier placed in front of an EDFA increases the overall gain bandwidth to 75 nm [16]. Rottwitt and Kidorf used two cascaded Raman lasers operating at different wavelengths to create an ultrawide-band Raman amplifier and realized a transparent window as wide as 92 nm for 45-km fiber span [17]. Authors proposed Raman amplifiers pumped with the so-called WDM pumping technique, in which 14XX-nm pump laser diodes are combined through WDM couplers to generate a very high pump power over a wide wavelength range [18]. The wide wavelength range of pump light results in a wide and flat composite gain spectrum of Raman amplifier [19], [20].

In conjunction with the Internet's exploding demands, the maturity of the pump sources has invoked resurgence of Raman amplifiers in WDM transmission systems. As was discussed with respect to Fig. 1, a distributed amplification improves optical signal-to-noise ratio (OSNR). In other words, a Raman amplifier increases power budget margin in system design. Then, the question is what this extra budget should be used for. One answer to this question is to enhance spectral efficiency and realize terabit-per-second transmission [21], [22]. Also, Raman amplifiers play an important role in transoceanic multi-terabit-per-second WDM transmission [23]. An interesting use of the power budget margin is to extend the fiber span distance between amplifiers up to 250 km [24], 140 km [25], and 160 km [26]. Some attempts have been made to increase the bit rate of single channel up to 320 Gb/s [27]. Hansen *et al.* [28] and Takachio *et al.* [29] demonstrated that four-wave mixing could be suppressed even in dispersion shifted fibers (DSF) by using Raman amplifiers. Kawakami *et al.* have shown that use of Raman amplifier could reduce the effect of self-phase modulation (SPM) in a dispersion managed line comprising single-mode fiber (SMF) and reverse dispersion fiber (RDF) [30], [31]. Bigo *et al.* achieved more than 5-Tb/s transmission capacity by using Raman amplifiers along with a technique called vestigial sideband (VSB) like filtering [32]. Garrett *et al.* have demonstrated that Raman amplifiers operate nearly as well as those in the lab, even though the field-deployed fiber cables contained many connectors causing reflections [33].

This paper concentrates on ultrabroad-band Raman amplifiers pumped and gain-equalized by WDM high-power laser diodes. Section II reviews the fundamentals of Raman amplifier. Section III introduces the key technologies for WDM pumping. Section IV develops design issues of WDM-pumped Raman amplifiers. Section V examines the effect of polarization states of pump light. Section VI demonstrates performances of WDM-pumped Raman amplifiers. They include ultrabroad-band operation in transmission fibers, low-noise operation in DCF, low-cost configuration using depolarizers, ultraflat gain operation, and high temperature stability. Section VII concludes this paper.

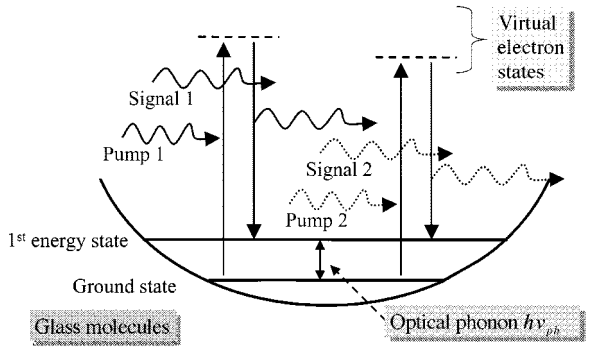

Fig. 2. Energy levels and transitions involved in stimulated Raman scattering.

II. Fundamentals of Raman Amplifier

Principle of Raman amplifier is based on the stimulated emission process associated with Raman scattering in fiber for amplification of signal. It is well known that silica-based optical fiber has Kerr nonlinearity. The finite response time of nonlinear polarization due to Kerr effect of medium results in energy loss of incident photon and excitation of molecule vibration or phonon. For silica, the response time is approximately on the order of 10 fs. Even though the response is very fast, the delay of nonlinear polarization with respect to the electric field of incident lightwave causes real vibration modes of silica fiber [34]. This process is classically described by imaginary part of nonlinear polarization, which causes absorption of incident wave and gain to Stokes shifted wave [35]. In quantum mechanics, it is described as a process in which an incident photon excites an electron to the virtual state and then the stimulated emission occurs when the electron de-excites down to the upper phonon energy level of glass molecule [36]. The energy levels and transitions involved in stimulated Raman scattering is depicted in Fig. 2. According to Fig. 2, the Stokes shift corresponds to the eigen-energy of a phonon, which is approximately 13.2 THz for optical fibers [4]. In Raman amplifiers, the signal wavelength is longer than the pump wavelength by the equivalent amount of frequency shift.

There are two kinds of phonons: one is acoustic phonon and the other is optical phonon. Raman scattering is the scattering between photon and optical phonon while that between photon and acoustic phonon is called Brillouin scattering. Because the optical phonon has almost uniform dispersion relation versus wave number, unlike stimulated Brillouin scattering, the phase matching is easily obtained for arbitrary relative directions between the pump and signal waves. Therefore, Raman amplifiers can take both co- and counterpump schemes [37]. Fig. 3 illustrates a general scheme of Raman amplifiers.

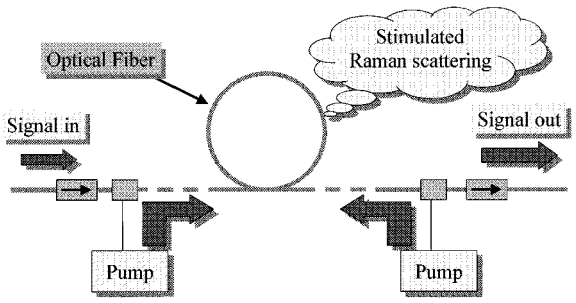

Fig. 3. General scheme of Raman amplifiers.

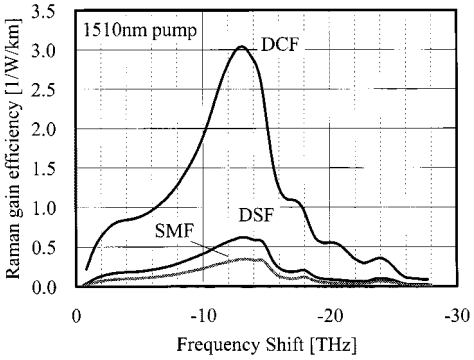

Fig. 4. Raman gain spectra for different fibers.

In a small signal regime where the pump depletion due to signal gain is neglected, the evolution of signal and pump power levels can be described respectively as the following rate equations:

$$\frac{dP_s}{dz} = \frac{g_R}{\lambda A_{\text{eff}}} P_p P_s - \alpha_s P_s$$
$$\frac{dP_p}{dz} = -\alpha_p P_p \tag{1}$$

where z is distance, P_s and P_p are signal and pump power levels, respectively, $g_R/\lambda A_{\text{eff}}$ is Raman gain coefficient, λ is pump wavelength, A_{eff} is effective area at pump wavelength, and α_s and α_p are attenuation coefficients at signal and pump wavelengths, respectively. This set of equations is easily solved and, thus, the Raman gain coefficient can be easily obtained.

As Stolen and Ippen observed [4], the Raman gain spectrum of optical fiber exhibits a broad continuum shape due to amorphous nature of the material. Fig. 4 plots Raman gain spectra for different fibers. The magnitude of the Raman gain is determined by nonlinearity, and the profile is determined by the respective fractions of GeO_2 and Silica [38]. Fig. 5 shows the normalized gain profile of three different fibers. The concentration of GeO_2 becomes larger in the order of SMF, DSF, and DCF.

It is of interest to compare Raman amplifier with EDFA. Even though the general schemes resemble each other except for the gain fiber, fundamental characteristics are in good contrast. One characteristic difference is the stimulated emission processes through either virtual or real energy states. The luminescence lifetime of Raman is in femtoseconds while that of EDFA is in milliseconds. The polarization state of lightwave is maintained during stimulated Raman scattering (SRS), while that is almost

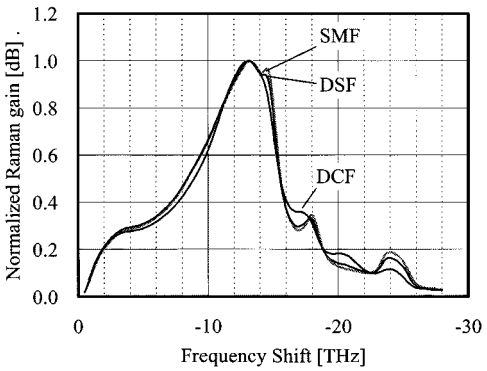

Fig. 5. Normalized gain profile of three different fibers.

completely depolarized in EDFA. Raman amplification is inherently of low noise regardless of pump level since the absorption of signal photon to the upper virtual state is extremely small, while in EDFA, a certain pump level has to be maintained in order to achieve the sufficient population inversion for low-noise operation. Temperature dependence of Raman gain spectrum is very small because of the off-resonant process and harmonic nature of optical phonons [39], [40], while that of EDFA is noticeable due to the temperature sensitivity of the local electric field created by glass molecules surrounding erbium ion [41], [42]. The temperature dependence will be discussed in Section VI-F).

Another characteristic difference between Raman amplifier and EDFA is either weak or strong interactions. Because Raman gain coefficient is considerably smaller than the gain coefficient of EDFA, the interaction lengths of both amplifiers are very different. Raman amplifier needs tens of kilometers of fiber, while EDFA uses only tens of meters of erbium-doped fiber (EDF), for comparable and sufficient amount of gain. Therefore, Raman amplifier is, in nature, distributed amplifier rather than lumped one. A drawback is then low efficiency. However, efficiency may not be an important issue in distributed amplifiers. If Raman amplifier had high efficiency, the pump would be depleted so rapidly in a short distance that it might not be a "distributed" amplifier anymore. As we have discussed in the previous section, a distributed amplifier is superior in terms of noise performance. Also, because of the low efficiency, most of pump power is lost mainly due to passive attenuation of optical fiber, and not due to the energy transfer to signal. This fact makes Raman amplifier almost ideal linear amplifier with high saturation power. For Raman amplifier with very fast luminescence lifetime, the linearity is essential to WDM application. In contrast, EDFA is efficient enough to have a low saturation power, which means EDFA is a quite nonlinear amplifier. However, since EDFA has very long luminescence lifetime, it is also viable for WDM transmissions. Thus, both Raman amplifier and EDFA are good for WDM transmissions in the opposite extremes. One important issue of concern due to long interaction length of Raman amplifier is the effect of double Rayleigh backscattering [43]. Without Raman amplification, Rayleigh-backscattered light attenuates out in long fiber span with loss. However, too much Raman gain gives rise to nondecaying Rayleigh-backscattered amplified spontaneous emission (ASE) and signal, which can Rayleigh

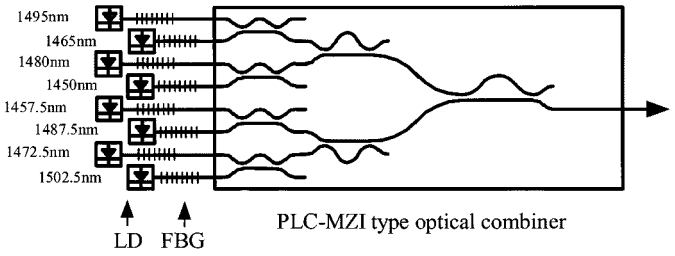

Fig. 6. Schematic diagram of WDM pumping.

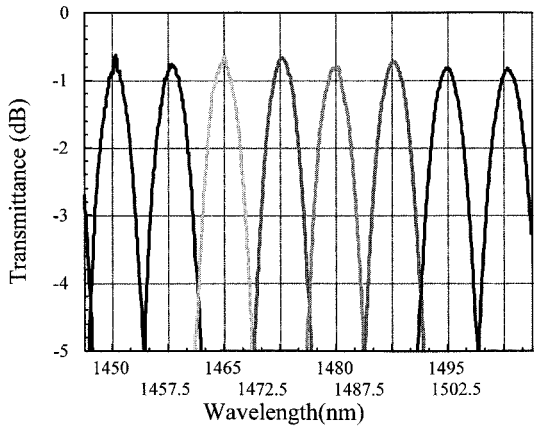

Fig. 7. Transmission spectra of PLC-MZI-WDM coupler.

backscatter again. This double-Rayleigh-backscattered portion of ASE and signal serves as noise for the original signal. Thus, there is an optimum amount of Raman gain [33].

The wide bandwidth of gain is a common aspect of both amplifiers, which also makes them convenient for WDM applications. The maturity of 14XX-nm pump laser diodes then readily leads us to realize practical broad-band Raman amplifiers for WDM purposes.

III. WDM Pumping for Raman Amplifiers

1480-nm pump laser diodes for EDFA have been matured [8] since completion of its development [7]. Authors have proposed "WDM" pumping technique to achieve a sufficient wide-band, and flat gain in Raman amplifiers [19], [20], [44]–[54]. The idea of "WDM" pumping is to prepare a set of pumps operating at different wavelengths combined through WDM couplers into a single fiber to realize a composite Raman gain. The composite Raman gain created by different wavelengths of pumps can be so designed as to be arbitrarily broad and flat.

For stable and efficient WDM pumping, pump lasers ought to have narrow and stable lasing spectra. Koyanagi *et al.* have achieved a very high power from fiber Bragg grating (FBG) stabilized pump laser diodes [11]. Tanaka *et al.* developed integrated imbalance Mach–Zehnder interferometers (MZIs) on a planar lightwave circuit (PLC) based on flame hydrolysis deposition (FHD) method [18]. Fig. 6 shows the schematic diagram of WDM pumping. Figs. 7 and 8 show the transmission spectra of PLC-MZI-WDM coupler, and pump laser output spectra without and with FBG stabilization, respectively. It is found from Figs. 7 and 8 that FBG stabilized spectrum fits in the

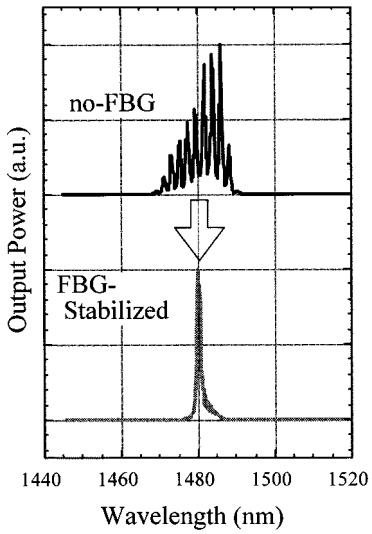

Fig. 8. Pump laser output spectra without and with FBG stabilization. (After [11].)

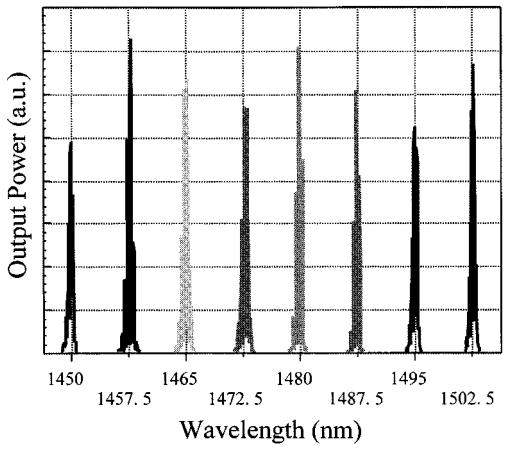

Fig. 9. Combined output optical spectrum of the WDM pump lasers.

transmission window of the coupler. Fig. 9 shows the combined output optical spectrum of the WDM pump lasers. The average insertion loss in this case was only 1.2 dB, and the maximum combined output power exceeded 1 W. Other different WDM coupler types, such as dielectric thin-film filter type, fused fiber coupler type, and so on, can also be used for the same purpose. Using this technique, one can design and realize Raman amplifiers with various gain shapes. This technique is also good for high-power EDFA [45].

IV. Design of WDM-Pumped Raman Amplifiers

The evolution of WDM pumps and signals are expressed in terms of the following equations [46]:

$$\frac{dP_\nu^{\pm}}{dz} = -\alpha_\nu P_\nu^{\pm} + \varepsilon_\nu P_\nu^{\mp} + P_\nu^{\pm} \sum_{\mu>\nu} \frac{g_{\mu\nu}}{A_\mu} (P_\mu^{+} + P_\mu^{-}) + 2h\nu \sum_{\mu>\nu} \frac{g_{\mu\nu}}{A_\mu} (P_\mu^{+} + P_\mu^{-})$$

$$\cdot \left[1+\frac{1}{\exp\left[\frac{h(\mu-\nu)}{kT}\right]-1}\right]$$
$$-P_\nu^{\pm}\sum_{\mu<\nu}\frac{\nu}{\mu}\frac{g_{\nu\mu}}{A_\nu}(P_\mu^{+}+P_\mu^{-})$$
$$-4h\nu P_\nu^{\pm}\sum_{\mu<\nu}\frac{g_{\nu\mu}}{A_\nu}\left[1+\frac{1}{\exp\left[\frac{h(\nu-\mu)}{kT}\right]-1}\right] \quad (2)$$

where subscripts μ and ν denote optical frequencies, superscripts $+$ and $-$ denote forward- and backward-propagating waves, respectively, P_ν is optical power within infinitesimal bandwidth around ν, α_ν is attenuation coefficient, ε_ν is Rayleigh-backscattering coefficient, A_ν is effective area of optical fiber at frequency ν, $g_{\mu\nu}$ is Raman gain parameter at frequency ν due to pump at frequency μ, h is Planck's constant, k is Boltzmann constant, and T is temperature. We note that g_R/λ in (1) is related to $g_{\mu\nu}$ in (2). In this equation, we include pump-to-pump, pump-to-signal, and signal-to-signal Raman interactions, pump depletions due to Raman energy transfer, Rayleigh backscattering, fiber loss, spontaneous emission noise and thermal noise. We have put a factor of two in the noise terms, the fourth and sixth terms, in (2). This is because spontaneous emission and thermal noise are not correlated with signal. Although the signal is polarized, the states of polarization (SOP) of signal and noise are scrambled and mixed together in the process of propagating through optical fiber.

For design of composite Raman gain, loss and gain terms are important. And because the noise associated with stimulated Raman scattering is low and saturation power is high, the noise terms are relatively small and unimportant. Rayleigh-backscattered light does not grow significantly in case of moderate pump power level, which is always the case for system of interest. We importantly found that the frequency dependence of effective area A_ν plays an important role for accurate design of composite Raman gain, especially when the pump band is wide (c.f. [57]). It is difficult to generally describe its dependence for various kinds of fibers. For the present purpose, we do not have to directly measure effective area A_ν. But instead, the property $g_{\mu\nu}/A_\nu$ has to be measured with respect to wavelength for each fiber under consideration. Table I shows some exemplary measured peak values of $g_{\mu\nu}/A_\nu$ at different wavelengths for SMF and DSF, from which we find the significance of accounting for its wavelength dependence in case of wide pump band. We also found that the normalized spectral profile of $g_{\mu\nu}$ does scarcely depend on pump wavelength.

Accordingly, for thorough designs, one needs to numerically solve (2). Fig. 10 shows the simulated pump power evolution along distance when five different wavelengths with 100 mW of each power level are simultaneously launched into fiber. From Fig. 10, it is seen that the longest wavelength acquires gain while the shortest one suffers from largest attenuation due to energy transfer to longer wavelengths via stimulated Raman scattering.

The composite Raman gain in this case is expressed as the logarithmic sum of each Raman gain created by each pump

TABLE I
PEAK VALUES OF RAMAN GAIN EFFICIENCY, $g_{\mu\nu}/A_\nu$ (1/W/km)

Pump wavelength (μm)	1.420	1.510
Standard single mode fiber	0.4277	0.3451
Dispersion shifted fiber	0.7612	0.6206

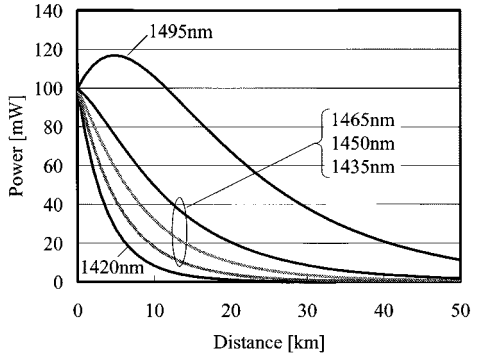

Fig. 10. Simulated pump power evolutions along distance. The fiber assumed is DSF.

wavelength with a weighting factor. The weighting factor is proportional to the area underneath the curve with respect to distance in Fig. 10. It is calculated by integrating the pump power level over distance. In this regard, the length of fiber is not important for the gain profile itself, or rather it only determines the amount of weighting factors by setting the upper limit of the integral to calculate the area. Likewise, the design procedure can be simplified. 1) One determines pump wavelengths with which a desired composite Raman gain can be obtained by adding in logarithmic scale individual Raman gain spectra shifted by the respective wavelength differences with adequate weighting factors. 2) One predicts how much power should be launched in order to realize the weighting factors through numerical simulations based on (2). Fig. 11 shows the comparison between the composite Raman gains calculated with weighting factors and experimentally realized by adjusting pump powers, where 11 pump channels are used. In this comparison, the simulated profile was simply created by adding the individual gain profiles weighted by appropriate factors. The agreement is superb.

A. Determination of Pumping Wavelength

The gain profile of a multiwavelength pumped Raman amplifier is expressed as a logarithmic superposition of the gain profiles pumped by respective pumping wavelengths. As already described in Section II, the shape of Raman gain pumped by a single wavelength is independent of the pumping wavelength as long as the peak value is normalized to be unity and the horizontal axis is expressed by the frequency shift from the pump. A possible gain profile of any pumping wavelength can be predicted from a gain profile pumped at a wavelength, though the magnitude of Raman gain is not determined only by the pumping wavelength. However, the predicted gain profile is sure to be realized by an appropriate pump power level unless it is beyond the limit. Therefore, the pumping wavelength allocation of a multiwavelength pumped Raman amplifier can be determined by adjusting the magnitude and position of respective gain profile so as to make the superposed profile a desirable one. Fig. 12

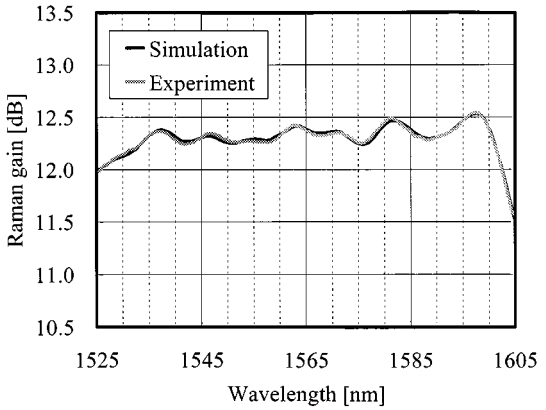

Fig. 11. Comparison between the composite Raman gains calculated with weighting factors and experimentally realized by adjusting pump powers. The fiber used was 25-km DSF.

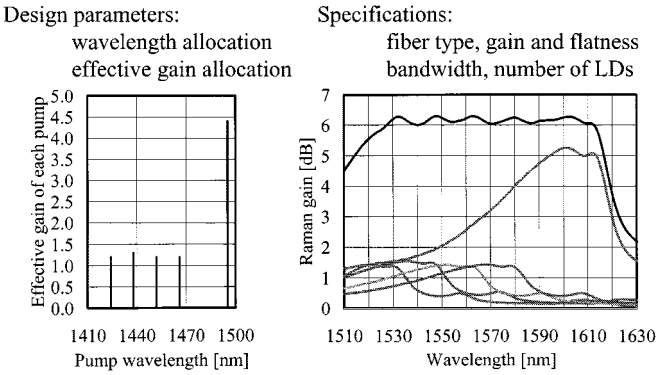

Fig. 12. Determination process of pumping wavelengths. The fiber assumed in this case is SMF.

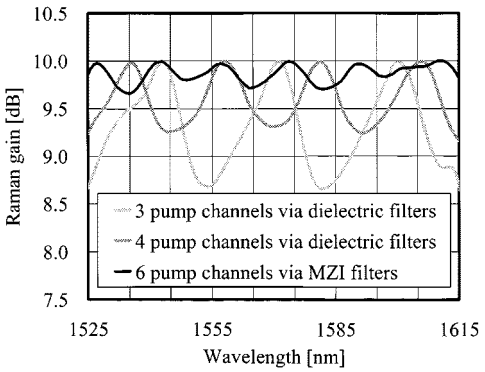

Fig. 13. Optimized design examples for C- plus L-band. The fiber assumed in this case is DSF.

illustrates the determination process of pumping wavelengths. The parameter "effective gain" corresponds to the magnitude of each gain profile in the right graph or the weighting factor as discussed above.

Fig. 13 shows optimized design examples for the wavelength range from 1525 nm to 1615 nm (C- plus L-band), where the peak levels of Raman gain are fixed to 10 dB in all cases. When the pumps are combined via dielectric filters, there is no restriction to choose the pumping wavelengths. In case of Mach–Zehnder interferometer (MZI) type wavelength multiplexer, the pumping wavelengths have to be on a grid with an equal frequency interval. The pumping wavelengths are determined so that the gain flatness is as small as possible. According to the results shown in Fig. 13, the number of local peaks corresponds to the number of pump channels and better gain flatness can be obtained by using the larger number of pumps.

A guideline to achieve a flat composite gain can be discussed as follows. Closely looking into the Raman gain spectra in Figs. 4 and 5, we find the profiles asymmetric around the gain peak. The spectra have a smoother and less steep curve toward smaller frequency shift from the peak. In order to create a flat top shape, we need to prepare a symmetrically opposite slope against this smoother gain slope by using many gain profiles laterally shifted with respect to each other. In other words, more gain profiles have to be so aligned as to create the opposite slope to the smoother slope of a gain profile located at a longest wavelength [44]. This guideline is actually applied to the example discussed in Sections VI-D and VI-E.

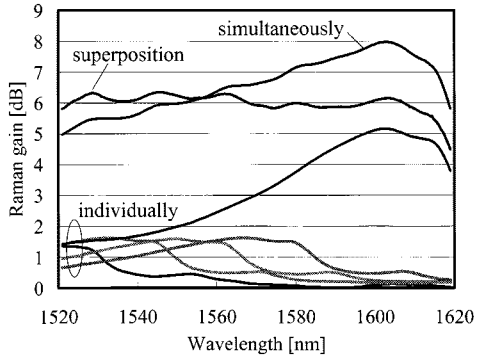

Fig. 14. Gain magnitude variation caused by pump-to-pump Raman interaction. The fiber used is 25-km DSF. Pump wavelengths are 1420, 1435, 1450, 1465, and 1495 nm with fiber launched powers of 61, 55, 48, 47, and 142 mW, respectively.

B. Determination of Pumping Power

The required pump power for a certain Raman gain is affected by several factors, such as Raman gain coefficient, polarization effect, fiber length, fiber loss at pump wavelength, pump depletion, and so on. In case of multiwavelength pumping scheme, the wavelength dependence of these factors is one of principal parameters to determine the pump power allocation. For example, Raman gain coefficient at shorter wavelength is larger than at longer, while fiber loss is generally larger at shorter wavelength due to Rayleigh scattering. Another important effect is pump-to-pump Raman interaction. It increases the required pumping power at shorter wavelength, because a longer wavelength pump absorbs the energy of shorter one. Fig. 14 shows the gain magnitude variation caused by pump-to-pump Raman interaction. There are the measured gain profiles individually pumped by each channel and simultaneously pumped by all channels. Numerical superposition of individually pumped gain profiles is also drawn in the figure. When the plural pumps with different wavelength are simultaneously launched into a fiber, the gain magnitudes created by the longer and shorter wavelength pumps increase and decrease, respectively.

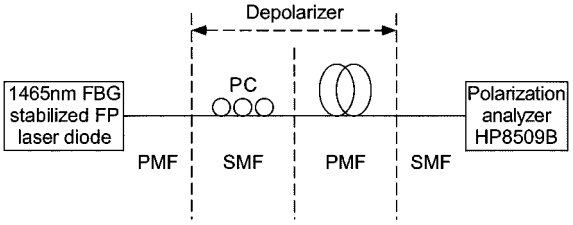

Fig. 15. Experimental setup of a depolarized pump LD.

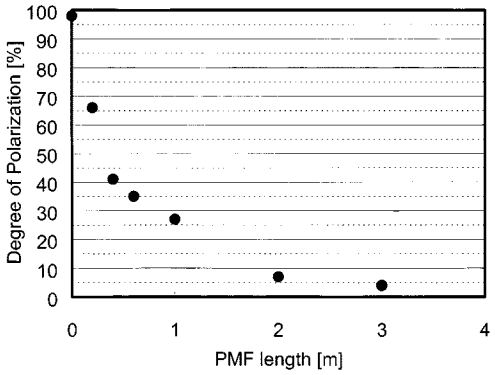

Fig. 16. Minimum DOP versus PMF length.

V. Degree of Polarization of Pump Laser and Polarization-Dependent Gain

Because the interaction lengths of Raman amplification are in general more than a few tens of kilometers, the correlation between the states of polarization (SOP) of signal and pump is lost during interactions. Therefore, even if the pump were polarized, the polarization dependence of Raman gain should be washed out. This is particularly the case in counterpumping scheme. However, there is still a statistical possibility that Raman gain can have polarization dependence. Since a LD has a linearly polarized output, polarization-combined LDs are usually used to offset the polarization dependent gain (PDG) of Raman amplifiers. This is convenient to obtain the higher pump power, but costly when the output power of a single LD is sufficiently large. Use of depolarizer to a pump LD is an alternative way to diminish PDG in Raman amplifiers. In this section, we demonstrate depolarization of a pump LD and show an experimental result of PDG versus degree of polarization (DOP) of the pump source, after [56].

Fig. 15 shows the experimental setup of a depolarized pump LD. Here, 1465-nm Fabry–Perot laser diode (FP-LD) stabilized by an FBG is depolarized through a depolarizer which consists of a polarization controller (PC) and a polarization maintaining fiber (PMF). The measured value of the output DOP of the PMF depends on the length and input SOP of the PMF. We measured the minimum DOP by adjusting the polarization controllers at the input end of the PMF. In principle, the linearly polarized beam emitted from LD has to be incident to the PMF exactly at 45° off of one of the eigen axes of the PMF. The reason why the PC was used here is to minimize the risk of errors in aligning the incident angle. For practical use, the output of LD should be through a PMF pigtail and it should be fusion-spliced to the depolarizer PMF at 45°. The error from 45° may result in partial incompleteness of depolarization. However, the depolarizer will be robust and stable. Fig. 16 shows the minimum DOP versus PMF length. As can be seen, the value of the DOP decreases to a few percent at 3 m, which is long enough with respect to the coherence length of the pump LD, and short enough to be low loss and cost.

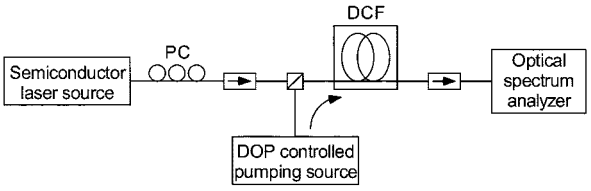

Fig. 17. Experimental setup for the measurement of PDG.

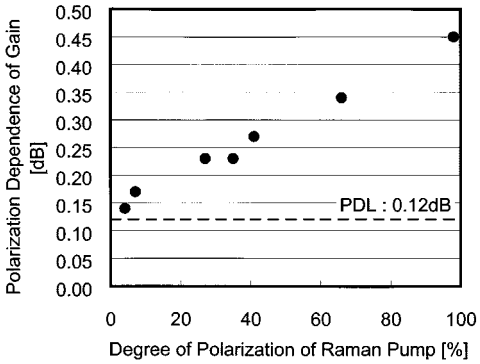

Fig. 18. Result of the measurement PDG versus DOP of the pump source.

Fig. 17 shows the experimental setup for the measurement of PDG. The DOP-controlled pump LD of 1465 nm and a semiconductor laser source of 1565 nm are used as the pump and signal, respectively. Co-propagating pumping is used, as larger PDG can be observed compared with counterpumping. A SOP of the signal was controlled using PC for measurement of PDG. Fig. 18 shows the result of the measurement PDG versus DOP of the pump source. When the DOP is 7%, PDG is almost equal to the value of polarization-dependent loss of the passive components. It represents that the PDG is sufficiently suppressed in this condition.

VI. Performances of WDM-Pumped Raman Amplifiers

A. Ultrawide-Band Operation [20], [55]

In this section, we demonstrate 100-nm bandwidth Raman amplifiers using 12-wavelength-channel WDM pump laser diode unit. The gain flatness is less than ± 0.5 dB, which is achieved through an asymmetric channel allocation of pump and without any gain equalization filters. Since the Raman gain shift is approximately 110 nm in 1550-nm signal window, we note that the bandwidth of 100 nm is the broadest limit of bandwidth in which crosstalk between pump and signal can be easily taken out.

Fig. 19 shows the schematic diagram of our 12-wavelength-channel WDM high power pump LD unit. We use high-power GRIN-SCH strained layer MQW BH laser diode modules. Each channel has polarization-multiplexed LDs using PBC. Each LD is stabilized by an FBG to have a narrow and stable spectrum for low insertion loss through the WDM coupler. The WDM coupler is a silica-based PLC comprising 11 MZIs.

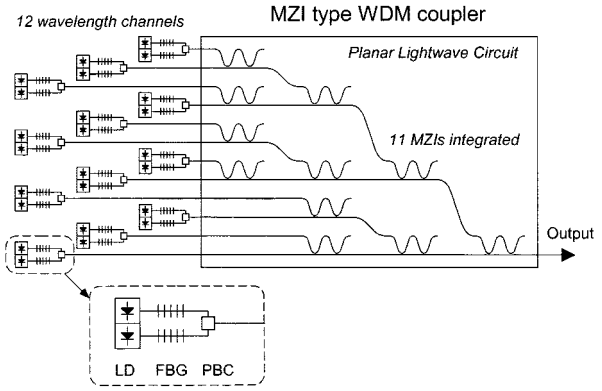

Fig. 19. Schematic diagram of our 12-wavelength-channel WDM high-power pump LD unit.

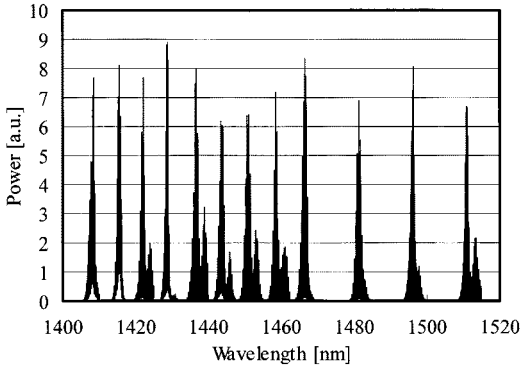

Fig. 20. The output spectrum of the pumping unit.

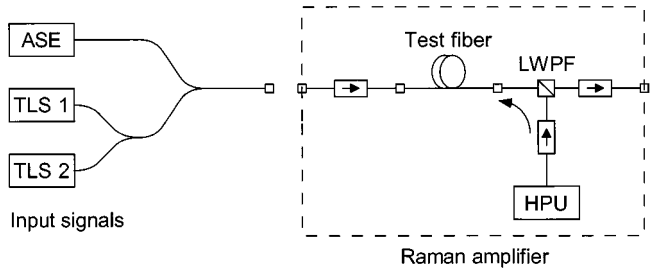

Fig. 21. Experimental setup of the broad-band Raman amplifiers.

Fig. 20 shows the output spectrum of the pumping unit. The insertion loss through PBC and WDM was typically 2.5 dB. The maximum total output power was more than 2.2 W. The channel spacing in the short wavelength section (1405–1457.5 nm) is 1 THz (∼7.5 nm) while that in the long one (1465–1510 nm) is 2 THz (∼15 nm).

Fig. 21 shows the experimental setup of the broad-band Raman amplifiers. Counterpropagating pumping is usually employed to avoid the pump-induced amplitude noise. The total insertion loss of the isolators and LWPF along the signal path is 1.6 dB at 1550 nm. The loss variation over 1520–1620-nm range is less than 1 dB. We use a broad-band ASE light source as the input signal as well as two tunable laser sources (TLS) used as probe signals to measure the gain profile.

We have tested three different types of fiber as Raman media: SMF, DSF, and RDF. Fig. 22 shows net gain profile of a 25-km SMF, a 25-km DSF, and a 20-km RDF, and launched pump

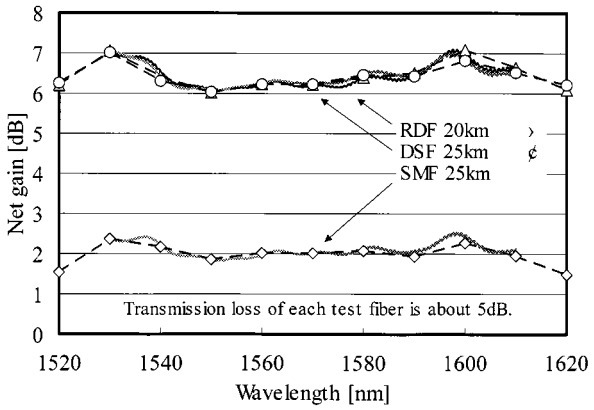

Fig. 22. Net gain profile of a 25-km SMF, a 25-km DSF, and a 20-km RDF.

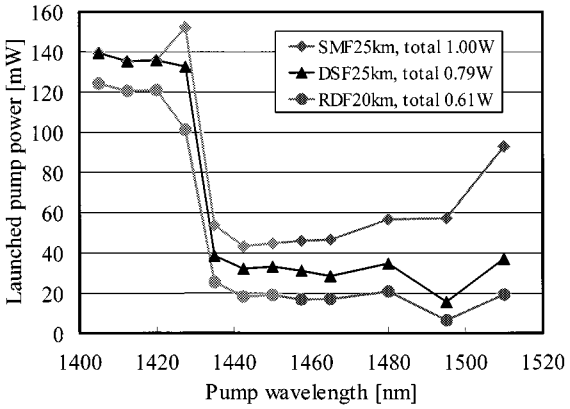

Fig. 23. Launched pump power of each channel.

power of each channel is shown in Fig. 23. The 100-nm net gain bandwidth with ±0.5 dB variations is obtained for all types of fibers. The average gain is 2 dB for SMF, 6.5 dB for DSF and RDF. The nonlinear refractive indexes divided by the effective areas are from small to large in the order of SMF, DSF, and RDF. Because Raman scattering cross section is larger for fibers with larger nonlinearity, RDF exhibits the highest pump-to-signal efficiency and the largest contrast in pump power distribution over channels due to pump-to-pump energy transfer. When the pump power in a longer wavelength becomes larger, the signal gain created by the pump at a shorter wavelength decreases. Hence, the maximum average gain is determined by the maximum pump power at shorter wavelengths as long as the gain has to be equalized by adjusting pump power distribution only.

It should be noted that in order to properly evaluate these Raman amplifiers, transmission experiments should be carried out especially with thorough assessment of noise properties at higher gain. However, accounting for many transmission experiments using distributed Raman amplifiers as reported in [21]–[29], [32], [33], Raman gain around 10 dB seems quite promising.

B. Low-Noise Operation in DCF for In-Line EDFA [19]

High-capacity D-WDM transmission systems based on existing standard single- mode fibers (SMF) require the use of dispersion-compensating fibers (DCF) [47]. In-line EDFAs for the such systems must have the gain to compensate the loss

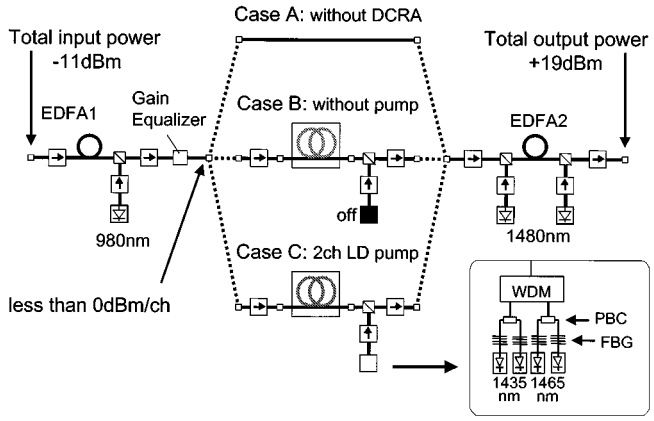

Fig. 24. Configurations of the three types of in-line amplifiers compared.

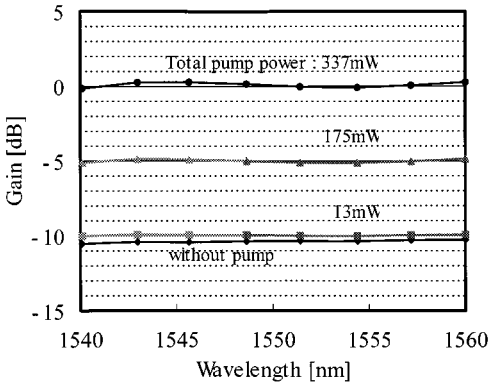

Fig. 25. Gain profile of DCRA at 0, −5, and −10 dB gain operations and without pumping.

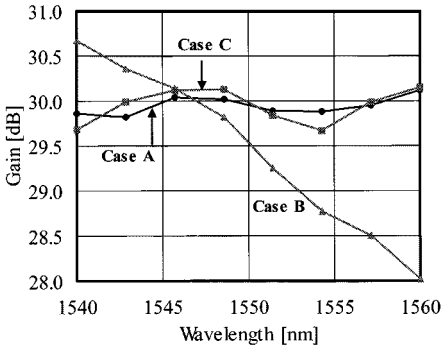

Fig. 26. Gain profiles of the three types of in-line amplifiers compared.

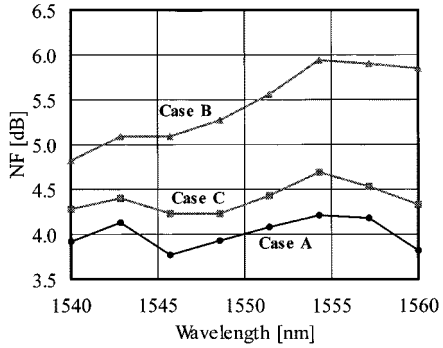

Fig. 27. Noise figure of the three types of in-line amplifiers compared.

due to both the transmission fibers and DCFs. The DCF is usually located between two cascaded EDFAs, in order to solve the tradeoff between SNR degradation and spurious nonlinear effects in the DCF [48]. For better systems, the in-line EDFAs should have lower noise figure (NF) and higher gain. However, one begins to face the above tradeoff when trying to improve the amplifier performance. In this section, we attempt to exploit Raman amplification for lower noise and higher gain of the amplifier, giving leeway for suppressing the nonlinear effects in the DCF. It was first demonstrated by Hansen *et al.* that the loss in DCF was compensated by Raman gain [49].

Fig. 24 shows the schematic diagram of the three types of in-line amplifiers compared. Case A represents two cascaded EDFAs without DCF, while case B and C have a dispersion compensating Raman amplifier (DCRA) between two stage EDFAs. The DCRA consists of a −1300 ps/nm DCF [50], isolators, a WDM coupler and a pumping unit that has 1435 nm and 1465 nm wavelength- and polarization-combined laser diodes. However, the unit does not operate in case B.

The EDFAs of the in-line amplifiers are designed as follows. Eight-channel WDM signals from 1540 to 1560 nm are used for the input signals. The input and output power of the first stage EDFA were set to be −20 dBm/ch and less than 0 dBm/ch, respectively. The first stage EDFA is pumped by a 980-nm laser diode to achieve low noise, while high-power 1480-nm laser diodes are used for the second. A gain equalizing filter is placed between the two stage EDFAs so that the in-line EDFA without interstage devices have 0.3-dB gain flatness at 30-dB gain operation over 20-nm bandwidth.

The gain profile of the DCRA was set to be flat at any gain level by adjusting the output power of each laser. Fig. 25 shows the gain profile of DCRA at 0, −5, and −10 dB gain operations and without pumping, where eight-channel WDM signals with −20 dBm/ch were launched into the DCRA. Total pump powers of each level are 337, 175, and 13 mW, respectively.

Fig. 26 shows the gain profile of each case. In case B, the gain tilts at 30 dB operation due to the increased intermediate loss of the DCRA, while the case C with the lossless DCRA does not have any gain tilt. Fig. 27 plots the NF of each case. It is clearly shown that the NF has improved by at most 1.5 dB for case C as compared with case B. This is simply explained: the intermediate loss aggravates the noise performance. The DCRA under lossless operation has the NF of 9–10 dB adding some noise resulting in approximately 0.5 dB increase in the NF, as compared with case A.

Last of all, we tested another in-line amplifier (case D), which is similar to case C but the pump for the DCRA is only polarization-combined 1450-nm laser diodes. Only five pump lasers are used in this in-line amplifier. The gain flatness of 1 dB at 30-dB operation and the NF of less than 4.7 dB were also achieved in this case, as shown in Fig. 28. There is no noticeable difference of the NF between case C and D, though the gain flatness is worse in case D than case C.

C. Low-Cost Pump Source for DCF [56]

In this section, we demonstrate a cost-effective pumping unit comprising only two LDs by using depolarized LD and optimizing pump wavelengths so as to obtain a sufficiently flat

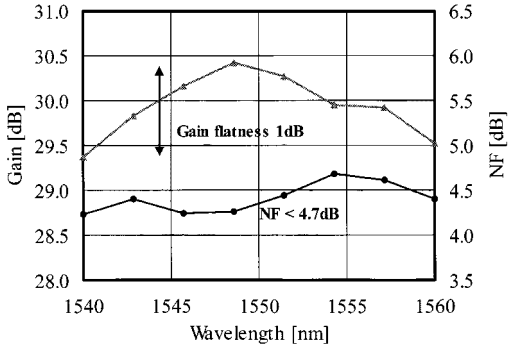

Fig. 28. Gain and noise figure in case D.

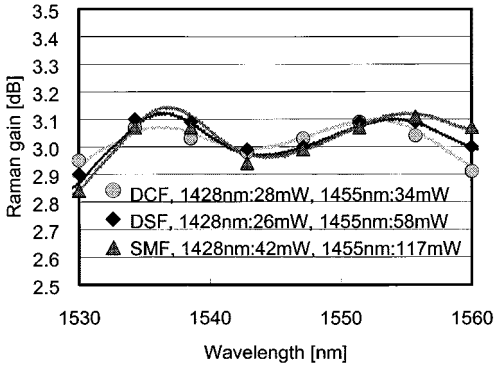

Fig. 29. Raman gain profiles of three types of fibers (DCF, DSF, SMF) pumped by the low-cost pump source.

Raman gain over the conventional EDFA gain band (C-band: 1530–1560 nm). As an example of the application, EDFA gain tilt is controlled by means of Raman gain in DCF instead of a variable optical attenuator (VOA) in an in-line amplifier [51], so that the gain flatness and output power can be simultaneously maintained constant against input power variations.

Fig. 29 shows the Raman gain profiles of three types of fibers (DCF, DSF, SMF) pumped by the low-cost pump source which consists of depolarized 1428- and 1455-nm FP-LDs with FBG. When DCF is the gain medium, the flatness of Raman gain is less than 0.2 dB. Although the unit is designed for the DCF, it is also available for other types of fibers such as SMF and DSF. Fig. 30 shows the Raman gain profiles of DCF at 3, 6, and 9 dB average gain operation. It should be noted the gain flatness is better than 0.5 dB in all cases, and that we only need a couple of less than 100 mW LDs to achieve 9 dB of Raman gain.

In order to keep the flatness against the gain variation of the amplifier, a VOA is usually used to control the overall gain of the amplifier with a constant gain EDFA. For the same purpose, Raman gain in a DCF can be used instead of the attenuation of a VOA. In this case, the noise figure of the amplifier can be improved by the virtue of reducing the DCF loss [19]. Fig. 31 shows the configuration of an in-line EDFA with DCF Raman amplified by the proposed unit. The loss of DCF is about 8 dB, including fiber splicing losses. In the following experiments, the average gain of the first stage EDFA and the total output power of the second stage EDFA are fixed at 14 dB and +14.5 dBm, respectively. The flatness is optimized at the condition that the input power and the Raman gain are −17 dBm/ch and 0 dB, respectively. Fig. 32 shows the total gain profile of the in-line amplifier against 6-dB input power variation. When only Raman gain compensates for the increase of the total gain of the amplifier, the gain profile remains flat. On the other hand, increasing the EDF gain alone without increasing Raman gain causes a significant gain tilt. On the contrary, we can make use of this behavior for active gain tilt control [52], [53]. Fig. 33 shows the demonstration of gain tilt control via Raman gain when the average gain of the amplifier is fixed at 25.5 dB. By partly replacing the EDFA gain with the Raman gain in the DCF, the gain tilt of the amplifier can be controlled. Using this scheme allows us to operate each individual amplifier at the optimum balance of the gain, flatness, and tilt with low noise.

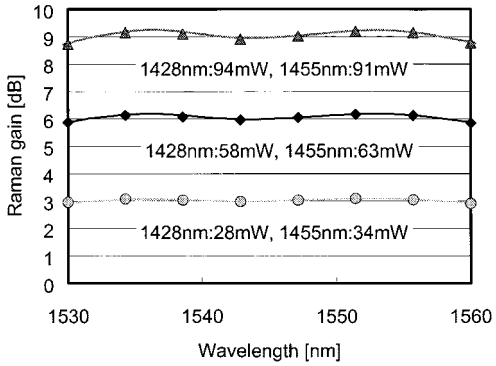

Fig. 30. Raman gain profiles of DCF at 3, 6, and 9 dB average gain operation.

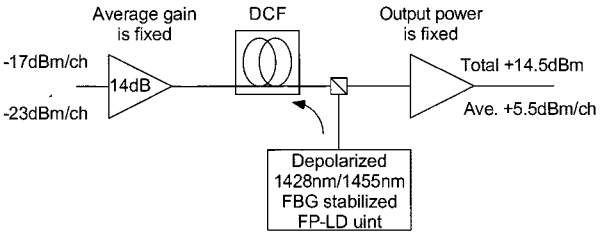

Fig. 31. Configuration of an in-line EDFA with DCF Raman amplified by the proposed unit.

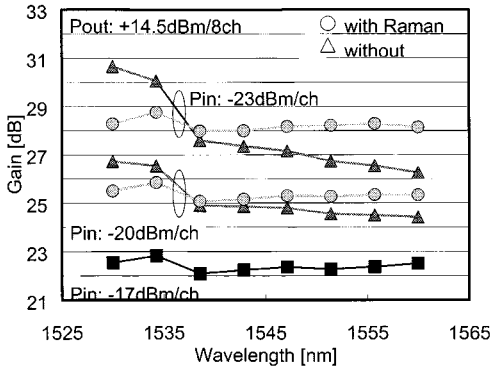

Fig. 32. Total gain profile of the in-line amplifier against 6-dB input power variation.

D. Upgradable Operation

In most cases, the number of WDM channels is gradually increased in the systems due to the gradual increase in bandwidth demand. In this context, the operating bands are also upgraded accordingly. For example, EDFAs operating in C-band are first

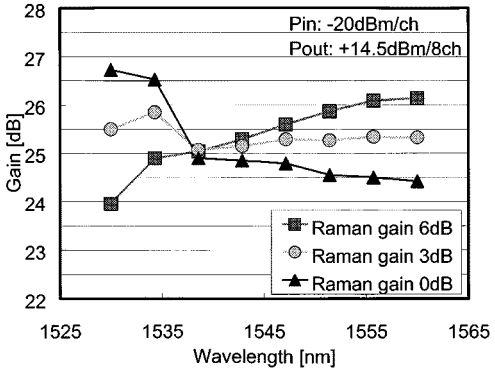

Fig. 33. Demonstration of gain tilt control via Raman gain.

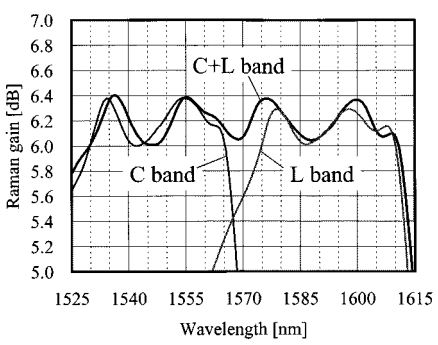

	Pump wavelength	Launched power
	nm	mW
C	1426	90
	1454	190
	total	280
L	1465	80
	1492	190
	total	270
C+L	1428	95
	1444	70
	1462	70
	1493	170
	total	405

Fig. 34. Calculated Raman gain spectra of C-, L-, and C-L-band Raman amplifiers with optimal sets of pumps. The fiber assumed is 50-km SMF.

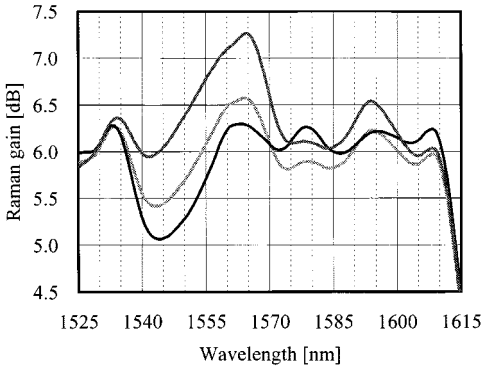

Fig. 35. Calculated Raman gain spectra of optimized C-L-band operations using the fixed set of pumps designed for individual C- and L-bands in Fig. 34. The fiber assumed is 50-km SMF.

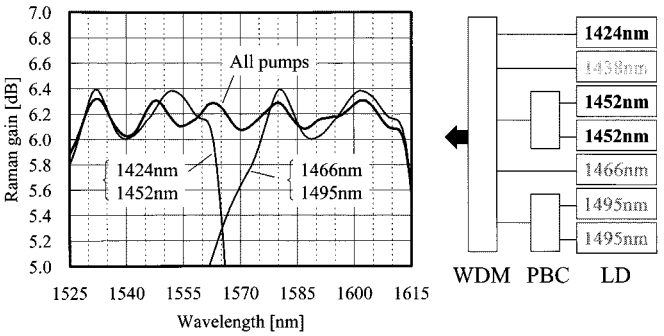

Fig. 36. Calculated Raman gain spectra of an upgradable Raman amplifier system with an *ad hoc* pump channel. The fiber assumed is 50-km SMF.

deployed and then those operating in L-band are additionally deployed later when needed. Similarly, it is desirable for Raman amplifiers to be upgradable from only C- to simultaneous C- and L-bands operations.

Fig. 34 shows the gain curves of practical examples of C- , L-, and C–L-band Raman amplifiers. Reasonable amount of gain and its flatness are achieved with a reasonable number of pump lasers with a commercially available amount of output powers. However, by comparing pump wavelengths for each case, they are all slightly different from each other. Each of C- and L-band Raman amplifiers cannot be used in the simultaneous operation of C- and L-bands. This means that this system is not upgradable and that they have to be wholly replaced when upgraded. Fig. 35 shows the optimal Raman gain achievable with simultaneous operation of C- and L-band Raman amplifiers instead of C–L-band Raman amplifier. The flatness is apparently not acceptable in regard with the performances of the other amplifiers.

We interestingly found that providing an *ad hoc* pump channel between the two shortest wavelengths can make system upgradable. The *ad hoc* channel is not used in individual band operations, but only turned on for C–L-band operation. This derives from the asymmetric profile of Raman gain spectra as was discussed in Section IV-A. The simultaneous operation of C- and L-band Raman amplifiers does not realize an asymmetric allocation of pump wavelengths. By adding an *ad hoc* pump channel, an asymmetrically allocated pump channels can only be realized for respective C-, L-, and C–L-bands. Fig. 36 shows an example in which an *ad hoc* pump channel is adopted. It is clear that this scheme provides a well-upgradable solution with a reasonable flatness maintained for all cases.

E. Ultraflat and Dynamic Gain-Tilt Operation [44]

In this section, we propose a multiwavelength pumping scheme where wavelength-multiplexed laser diodes on a 1-THz spaced grid are used, and demonstrate it is capable of 0.1-dB Raman gain flatness over the C- plus L-band (1527–1607 nm) without any gain flattening filters. By using this pumping scheme, we also demonstrate a smooth gain tilt to compensate for intersignal Raman tilt.

Fig. 37 shows a simulated broad-band Raman gain profile illustrating how the superposition of one-wavelength-pumped gain profiles shifted by the pump frequency difference can create a flattened gain profile. In this simulation, adequate 11 channels among the 16 frequencies in Fig. 38 are used. We assume the use of DSF for Raman fiber.

In Fig. 37, the curve A, B, and C represent the total Raman gain of 11 channels, the sum of nine channels in the shorter wavelength range, and that of two in the longer range, respectively. The 1-THz-spaced gain curves having almost same and small peak levels are so added as to obtain a smooth slope like curve B. Since curve C has an opposite slope of curve B, the total gain profile A is flattened. This example demonstrates that 0.1-dB flatness can be achieved by using this scheme.

We prepare a pumping unit comprising 12 wavelength channels in the range of 212.2–199.3 THz (1412.5–1504.5 nm) on a 1-THz-spaced grid, where the source of each channel is a

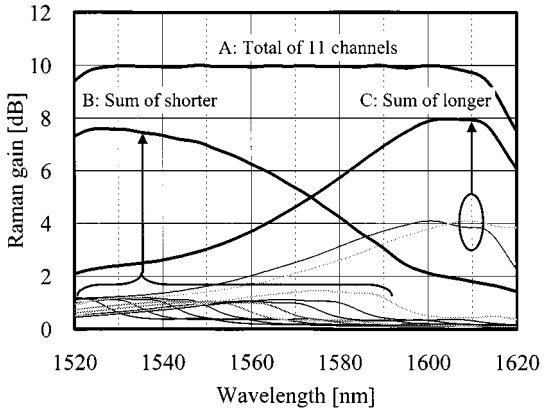

Fig. 37. Simulated broad-band Raman gain profile. The fiber is assumed to be DSF.

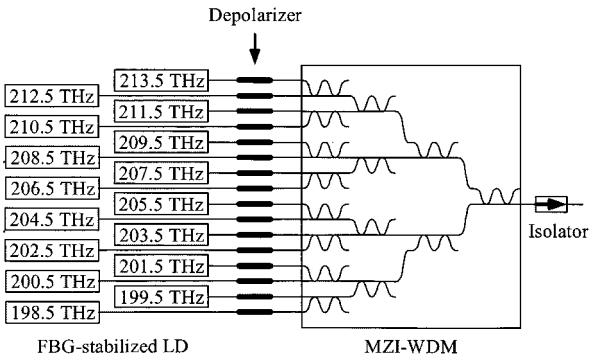

Fig. 38. Concept of 1-THz spaced multiwavelength pumping unit.

high-power GRIN-SCH strained layer MQW BH laser diode module.

Fig. 39 shows the measured Raman gain profile and the launched pump power of each channel. In this experiment, a 25-km DSF is used as Raman fiber with counterpropagating pump configuration. The gain flatness is about 0.1 dB over the wavelength range of the C- plus L-band (1527–1607 nm). Although the prepared unit has different absolute pumping frequencies from those in Fig. 38, the obtained flatness is as small as simulated in Fig. 37. This is because the relative frequencies were comparable to realize the almost same flatness. The average Raman gain is almost 10.5 dB, which can compensate for an approximately 50-km transmission fiber. Because of the pump-to-pump interaction, the launched powers of lower frequency pumps are made smaller in order to flatten the gain profile. In other words, the maximum available Raman gain in this scheme is determined by the maximum output power of higher frequency pumps.

This multiwavelength pumping scheme can create a very flexible Raman gain profile. A smooth tilted profile can also be formed as shown in Fig. 40, where the gain by the lower frequency pumps are decreased and the others are adjusted so as to shape various slanted straight profiles. An intersignal Raman tilt in broad-band WDM transmission can be canceled by using this pumping scheme.

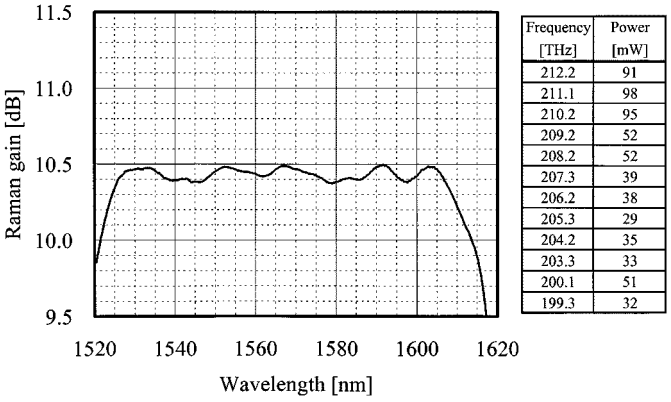

Frequency [THz]	Power [mW]
212.2	91
211.1	98
210.2	95
209.2	52
208.2	52
207.3	39
206.2	38
205.3	29
204.2	35
203.3	33
200.1	51
199.3	32

Fig. 39. Measured Raman gain profile and the launched pump power of each channel. The fiber is 25-km DSF.

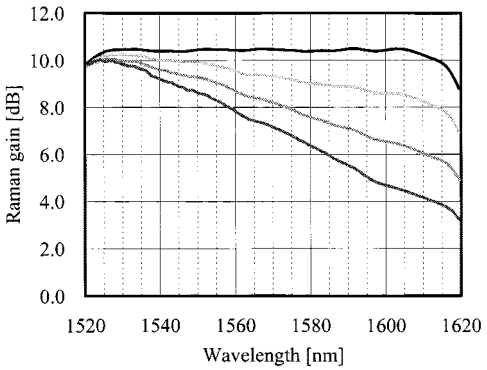

Fig. 40. Demonstration of various slanted straight profile. The fiber is 25-km DSF.

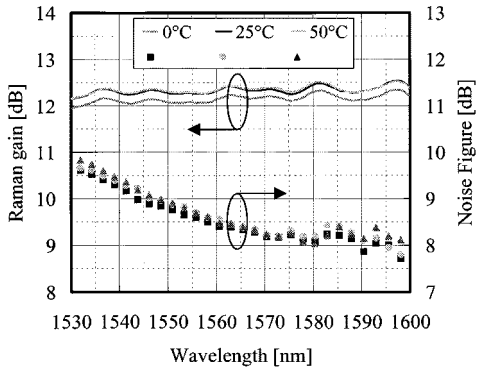

Fig. 41. Temperature dependence on Raman gain and noise figure. The fiber is 25-km DSF.

F. Temperature Stability

Fig. 41 shows the temperature dependence on Raman gain and noise figure in the broad-band Raman amplifier. The launched pump power of each wavelength channel is maintained through the experiment and the only amplifier fiber is put into a thermal chamber. The variation due to temperature is less than 0.5 dB for both gain and noise figure. The small reduction of Raman gain at 0 °C may be derived from microbending loss of pumps. The temperature stability of Raman gain is magnificent.

VII. Conclusion

This paper reviewed recent progress in broad-band Raman amplifiers for WDM transmissions. The fundamentals of Raman amplifier are discussed in contrast to erbium-doped fiber amplifiers to show excellent applicability of both amplifiers to WDM transmissions in the opposite extremes. A new technique called "WDM pumping" was introduced to obtain sufficient, ultrabroad, and flat gain in Raman amplifiers only using WDM diode pumps. We have developed the design issues of this technique, introducing superposition rule and account for pump-to-pump energy transfer. This design rule was demonstrated to realize outstanding performances such as 100 nm of flat gain bandwidth, 0.1 dB flatness over 80 nm.

The maximum available Raman gain using this scheme will be increased in accordance with the increasing output power of pump lasers. Then, other limiting factors such as double-Rayleigh-scattering noise may become important [33]. However, the detailed studies in case of WDM pumping based on diode lasers have yet to be conducted.

Acknowledgment

The authors would like to thank Ms. S. Kado for comparing numerical calculations with experiments, Dr. M. Sakano for fruitful discussions on modeling, and Mr. T. Ninomiya for his support.

References

[1] A. Srivastava, Y. Sun, J. W. Sulhoff, C. Wolf, M. Zirngibl, R. Monnard, A. R. Chraplyvy, A. A. Abramov, R. P. Espindola, T. A. Strasser, J. R. Pedrazzani, A. M. Vengsarkar, J. L. Zyskind, J. Zhou, D. A. Ferrand, P. F. Wysocki, J. B. Judkins, and Y. P. Li, "1 Tb/s transmission of 100 WDM 10 Gb/s channels over 400 km TrueWaveTM fiber," in *Proc. Optical Fiber Communication Conf. 1998*, Paper PD10.

[2] S. Aisawa, T. Sakamoto, M. Fukui, J. Kani, M. Jinno, and K. Oguchi, "Ultra-wide band, long distance WDM transmission demonstration: 1 Tb/s (50×20 Gb/s), 600 km transmission using 1550 and 1580 nm wavelength bands," in *Proc. Optical Fiber Communication Conf. 1998*, Paper PD11.

[3] D. Le Guen, S. Del Burgo, M. L. Moulinard, D. Grot, M. Henry, F. Favre, and T. Georges, "Narrow band 1.02 Tbit/s (51×20 Gbit/s) soliton DWDM transmission over 1000 km of standard fiber with 100 km amplifier spans," in *Proc. Eur. Conf. Optical Communication*, 1998, Paper PD4.

[4] R. H. Stolen and E. P. Ippen, "Raman gain in glass optical waveguides," *Appl. Phys. Lett.*, vol. 22, pp. 276–278, 1973.

[5] Y. Aoki, S. Kishida, K. Washio, and K. Minemura, "Bit error rate evaluation of optical signals amplified via stimulated Raman process in an optical fiber," *Electron. Lett.*, vol. 21, no. 5, pp. 191–193, 1985.

[6] L. F. Mollenauer, J. P. Gordon, and M. N. Islam, "Soliton propagation in long fibers with periodically compensated loss," *J. Quantum Electron.*, vol. QE-22, pp. 157–173, Jan. 1986.

[7] S. Namiki, Y. Ikegami, Y. Shirasaka, and I. Oh-ishi, "Highly coupled high power pump laser modules," in *Proc. Optical Amplifiers and Their Applications*, 1993, Paper MD5.

[8] T. Kimura, N. Tsukiji, A. Iketani, N. Kimura, H. Murata, and Y. Ikegami, "High temperature operation quarter watt 1480 nm pump LD module," in *Proc. Optical Amplifiers and Their Applications*, 1999, Paper ThD12.

[9] E. Desurvire, *Erbium-Doped Fiber Amplifiers*. New York: Wiley, 1994.

[10] P. C. Becker, N. A. Olsson, and J. R. Simpson, *Erbium-Doped Fiber Amplifiers*. New York: Academic, 1999.

[11] S. Koyanagi, A. Mugino, T. Aikiyo, and Y. Ikegami, "The ultra high-power 1480 nm pump laser diode module with fiber Bragg grating," in *Proc. Optical Amplifiers and Their Applications*, 1998, Paper MC2.

[12] A. Kasukawa, "High power 980 nm and 1480 nm lasers," in *Proc. Optical Amplifiers and Their Applications*, 2000, Paper OMC1.

[13] S. G. Grubb, S. T. A, W. Y. Cheung, W. A. Reed, V. Mizrahi, T. Erdogan, P. J. Lemaire, and A. M. Vengsarkar, "High-power 1.48 μm cascaded Raman laser in germanosilicate fibers," in *Proc. Optical Amplifiers and Their Applications*, 1995, Paper SaA4.

[14] P. B. Hansen, L. Eskildsen, S. G. Grubb, A. J. Stentz, T. A. Strasser, J. Judkins, J. J. DeMarco, R. Pedrazzani, and D. J. DiGiovanni, "Capacity upgrades of transmission systems by Raman amplification," *IEEE Photon. Technol. Lett.*, vol. 9, no. 2, pp. 262–264, 1997.

[15] M. Nissov, C. R. Davidson, K. Rottwitt, R. Menges, P. C. Corbett, D. Innis, and N. S. Bergano, "100 Gb/s (10×10 Gb/s) WDM transmission over 7200 km using distributed Raman amplification," in *Proc. Eur. Conf. Optical Communication*, vol. 5, 1997, pp. 9–12.

[16] H. Masuda, S. Kawai, K. Suzuki, and K. Aida, "75-nm 3-dB gain-band optical amplification with erbium-doped fluoride fiber amplifiers and distributed Raman amplifiers in 9×2.5-Gb/s WDM transmission," in *Proc. Eur. Conf. Optical Communication*, vol. 5, 1997, pp. 73–76.

[17] K. Rottwitt and H. D. Kidorf, "A 92 nm bandwidth Raman amplifier," in *Proc. Optical Fiber Communication Conf.*, 1998, Paper PD6.

[18] K. Tanaka, K. Iwashita, Y. Tashiro, S. Namiki, and S. Ozawa, "Low-loss integrated Mach–Zehnder interferometer-type eight-wavelength multiplexer for 1480-nm band pumping," in *Proc. Optical Fiber Communication Conf.*, 1999, Paper TuH5.

[19] Y. Emori, Y. Akasaka, and S. Namiki, "Less than 4.7 dB noise figure broadband in-line EDFA with a Raman amplified -1300 ps/nm DCF pumped by multi-channel WDM laser diodes," in *Proc. Optical Amplifiers and Their Applications*, 1998, Paper PD3.

[20] Y. Emori and S. Namiki, "100 nm bandwidth flat gain Raman amplifiers pumped and gain-equalized by 12-wavelength-channel WDM high power laser diodes," in *Proc. Optical Fiber Communication Conf.*, 1999, Paper PD19.

[21] T. N. Nielsen, A. J. Stentz, P. B. Hansen, Z. J. Chen, D. S. Vengsarkar, T. A. Strasser, K. Rottwitt, J. H. Park, S. Stulz, S. Cabot, K. S. Feder, P. S. Westbrook, and S. G. Kosinski, "1.6Tb/s (40×40 Gb/s) transmission over 4×100 km nonzero-dispersion fiber using hybrid Raman–Erbium-doped inline amplifiers," in *Proc. Eur. Conf. Optical Communication*, 1999, Postdeadline paper, pp. 26–27.

[22] H. Suzuki, J. Kani, H. Masuda, N. Takachio, K. Iwatsuki, Y. Tada, and M. Sumida, "25 GHz-spaced, 1 Tb/s (100×10 Gb/s) super dense-WDM transmission in the C-band over a dispersion-shifted fiber cable employing distributed Raman amplification," in *Proc. Eur. Conf. Optical Communication*, 1999, Postdeadline paper, pp. 30–31.

[23] T. Tanaka, N. Shimojoh, T. Naito, H. Nakamoto, I. Yokota, T. Ueki, A. Sugiyama, and M. Suyama, "2.1-Tbit/s WDM transmission over 7221 km with 80-km repeater spacing," in *Proc. Eur. Conf. Optical Communication*, 2000, Postdeadline paper 1.8.

[24] J. P. Blondel, F. Boubal, E. Brandon, L. Buet, L. Labrunie, P. Le Roux, and D. Toullier, "Network application and system demonstration of WDM systems with very large spans (Error-free 32×10 Gbit/s 750 km transmission over 3 amplified spans of 250 km)," in *Proc. Optical Fiber Communication Conf.*, 2000, Paper PD31.

[25] T. Terahara, T. Hoshida, J. Kumasako, and H. Onaka, "128×10.66 Gbit/s transmission over 840-km standard SMF with 140-km optical repeater spacing (30.4-dB loss) employing dual-band distributed Raman amplification," in *Proc. Optical Fiber Communication Conf.*, 2000, Paper PD28.

[26] Y. Zhu, W. S. Lee, C. Scanhill, C. Fludger, D. Watley, M. Jones, J. Homan, B. Shaw, and Hadjifotiou, "1.28 Tbit/s (32×40 Gbit/s) transmission over 1000 km with only 6 spans," in *Proc. Eur. Conf. Optical Communication*, 2000, Postdeadline paper 1.4.

[27] G. Raybon, B. Mikkelsen, R. J. Essiambre, A. J. Stentz, T. N. Nielsen, D. W. Peckham, L. Hsu, L. Gruner-Nielsen, K. Dreyer, and J. E. Johnson, "320 Gbit/s single-channel pseudo-linear transmission over 200 km of nonzero-dispersion fiber," in *Proc. Optical Fiber Communication Conf.*, 2000, Paper PD29.

[28] P. B. Hansen, A. Stentz, T. N. Nielsen, R. Espindola, L. E. Nelson, and A. A. Abramov, "Dense wavelength-division multiplexed transmission zero-dispersion DSF by means of hybrid Raman–Erbium-doped fiber amplifiers," in *Proc. Optical Fiber Communication Conf.*, 1999, Paper PD8.

[29] N. Takachio, H. Suzuki, H. Masuda, and M. Koga, "32×10 Gb/s distributed Raman amplification transmission with 50 GHz channel spacing in the zero-dispersion region over 640 km of 1.55-mm dispersion-shifted fiber," in *Proc. Optical Fiber Communication Conf.*, 1999, Paper PD9.

[30] H. Kawakami, Y. Miyamoto, K. Yonenaga, and H. Toba, "Highly efficient distributed Raman amplification system in a zero-dispersion-flattened transmission line," in *Proc. Optical Amplifiers and Their Applications*, 1999, Paper ThB5.

[31] K. Mukasa, Y. Akasaka, Y. Suzuki, and T. Kamiya, "Novel network fiber to manage dispersion at 1.55 mm with combination of 1.3 mm zero dispersion single mode fiber," in *Proc. Eur. Conf. Optical Communication*, vol. 1, 1997, pp. 127–130.

[32] S. Bigo, A. Bertaina, Y. Frignac, S. Borne, L. Lorcy, D. Hamoir, D. Bayart, J. P. Hamaide, W. Idler, E. Lach, B. Franz, G. Veith, P. Sillard, L. Fleury, P. Guenot, and P. Nouchi, "5.12 Tbit/s (128 × 40 Gbit/s WDM) transmission over 3 × 100 km of TeraLight™TM fiber," in *Proc. Eur. Conf. Optical Communication*, 2000, Postdeadline paper 1.2.

[33] L. D. Garrett, M. Eiselt, and R. W. Tkach, "Field demonstration of distributed Raman amplification with 3.8 dB Q-improvement for 5 × 120 km transmission," in *Proc. Optical Fiber Communication Conf.*, 2000, Paper PD42.

[34] R. H. Stolen, J. P. Gordon, W. J. Tomlinson, and H. A. Haus, "Raman response function of silica-core fibers," *J. Opt. Soc. Amer. B*, vol. 6, no. 6, pp. 1159–1166, 1989.

[35] R. W. Boyd, *Nonlinear Optics*. New York: Academic, 1992, pp. 365–379.

[36] E. G. Sauter, *Nonlinear Optics*. New York: Wiley, 1996, pp. 77–88.

[37] K. Okamoto, *Theory of Optical Waveguides*. Tokyo, Japan: Corona, 1992, pp. 191–198.

[38] F. Galeener, J. Millelsen, R. Geils, and W. Mosby, "The relative Raman cross sections of vitreous SiO_2, GeO_2, B_2O_3 and P_2O_5," *Appl. Phys. Lett.*, vol. 32, pp. 34–36, 1978.

[39] S. A. E. Lewis, S. V. Chernikov, and J. R. Taylor, "Temperature-dependent gain and noise in fiber Raman amplifiers, *Opt. Lett.*, vol. 24, no. 24, pp. 1823–1825, 1999.

[40] S. Namiki and Y. Emori, "Broadband Raman amplifiers design and practice," *Proc. Optical Amplifiers and Their Applications*, pp. 7–9, 2000.

[41] N. Kagi, A. Oyobe, and K. Nakamura, "Temperature dependence of the gain in erbium doped fibers," *J. Lightwave Technol.*, vol. 9, pp. 261–265, 1991.

[42] T. Tsuda, M. Miyazawa, K. Nishiyama, T. Ota, K. Mizuno, Y. Mimura, Y. Tashiro, Y. Emori, and S. Namiki, "Gain-flattening filters with autonomous temperature stabilization of Erbium gain," in *Proc. Optical Amplifiers and Their Applications*, 2000, Paper OWA4, pp. 173–175.

[43] P. B. Hansen, L. Eskildsen, A. J. Stentz, T. A. Strasser, J. Judkins, J. J. DeMarco, R. Pedrazzani, and D. J. DiGiovanni, "Rayleigh scattering limitations in distributed Raman pre-amplifiers," *IEEE Photon. Technol. Lett.*, vol. 10, no. 1, pp. 159–161, 1998.

[44] Y. Emori, S. Matsushita, and S. Namiki, "1-THz-spaced multi-wavelength pumping for broadband Raman amplifiers," in *Proc. Eur. Conf. Optical Communication*, vol. 2, 2000, Paper 4.4.2., pp. 73–74.

[45] Y. Tashiro, S. Koyanagi, K. Aiso, and S. Namiki, "1.5 W erbium doped fiber amplifier pumped by the wavelength division-multiplexed 1480 nm laser diodes with fiber Bragg grating," *Proc. Optical Amplifiers and their Applications*, 1998.

[46] M. Sakano, A. Aikawa, and S. Namiki, , submitted for publication.

[47] J. M. Dugan, A. J. Price, M. Ramadan, D. L. Wolf, E. F. Murphy, A. J. Antos, D. K. Smith, and D. W. Hall, "All-optical, fiber-based 1550 nm dispersion compensation in a 10 Gbit/s, 150 km transmission experiment over 1310 nm optimized fiber," in *Proc. Optical Fiber Communication Conf.*, 1992, Paper PD14.

[48] C. D. Chen, J.-M. P. Delavaux, B. W. Hakki, O. Mizuhara, T. V. Nguyen, R. J. Nuyts, K. Ogawa, Y. K. Park, R. E. Tench, L. D. Tzeng, and P. D. Yeates, "Field experiment of 10 Gb/s, 360 km transmission through embedded standard (non-DSF) fiber cables," *Electron. Lett.*, vol. 30, pp. 1159–1160, 1994.

[49] P. B. Hansen, G. Jacobovitz-Veselka, L. Grüner-Nielsen, and A. J. Stentz, "Raman amplification for loss compensation in dispersion compensating fiber modules," *Electron. Lett.*, vol. 34, pp. 1136–1137, 1998.

[50] Y. Akasaka, R. Sugisaki, and T. Kamiya, "Dispersion compensating technique of 1300 nm zero-dispersion SM fiber to get flat dispersion at 1550 nm," in *Proc. Eur. Conf. Optical Communication*, vol. 2, 1995, pp. 605–608.

[51] S. Kinoshita, C. Ohshima, H. Itoh, M. Takeda, T. Kobayashi, Y. Sugaya, T. Okiyama, and T. Chikama, "Wide-dynamic-range WDM optical fiber amplifiers for 32 × 10 Gb/s, SMF transmission systems," in *Proc. Optical Amplifiers and Their Applications*, 1998, Paper WA2.

[52] T. Naito, T. Terahara, N. Fukushima, N. Shimojoh, T. Tanaka, and M. Suyama, "Active gain slope compensation in large-capacity, long-haul WDM transmission system," in *Proc. Optical Amplifiers and Their Applications*, 1999, Paper WC5.

[53] M. Takeda, S. Kinoshita, Y. Sugaya, and T. Tanaka, "Active gain-tilt equalization by preferentially 1.43μm- or 1.48μm-pumped Raman amplification," in *Proc. Optical Amplifiers and Their Applications*, 1999, Paper ThA3.

[54] Y. Emori, Y. Akasaka, and S. Namiki, "Broadband lossless DCF using Raman amplification pumped by multichannel WDM laser diodes," *Electron. Lett.*, vol. 34, pp. 2145–2146, 1998.

[55] Y. Emori, K. Tanaka, and S. Namiki, "100 nm bandwidth flat-gain Raman amplifiers pumped and gain-equalised by 12-wavelength-channel WDM laser diode unit," *Electron. Lett.*, vol. 35, pp. 1355–1356, 1999.

[56] Y. Emori, S. Matsushita, and S. Namiki, "Cost-effective depolarized diode pump unit designed for C-band flat-gain Raman amplifiers to control EDFA gain profile," *Proc. Optical Fiber Communication Conf.*, 2000.

[57] H. Kidorf, K. Rottwitt, M. Nissov, M. Ma, and E. Rabarijaona, "Pump interactions in a 100-nm bandwidth Raman amplifier," *IEEE Photon. Technol. Lett.*, vol. 11, pp. 530–532, 1999.

Shu Namiki received B.E., M.S., and Dr. Sci. degrees in physics and applied physics from Waseda University in 1986, 1988, and 1998, respectively.

He joined Furukawa Electric Co., Ltd. in 1988 where he has developed award-winning high-power pump laser packaging technologies. From 1994 to 1997, he was a Visiting Scientist at the optics group of the Research Laboratory of Electronics, Massachusetts Institute of Technology, where he studied on nonlinear solitary waves in fibers. His current position is to develop next generation devices as a manager of Optical Transmission Systems Group, Fitel Photonics Laboratory, Furukawa Electric Co., Ltd., Ichihara, Japan.

Dr. Namiki is a member of the Optical Society of America and the Institute of Electronics, Information and Communication Engineers.

Yoshihiro Emori received B.E., M.E., and Dr.Eng. degrees in electrical and electronic engineering from the Tokyo Institute of Technology in 1992, 1994, and 1997, respectively.

He joined Furukawa Electric Co., Ltd., Ichihara, Japan, in 1997 where he has developed erbium-doped fiber amplifiers and Raman amplifiers for WDM transmission systems.

Dr. Emori is a member of the Optical Society of America and the Institute of Electronics, Information and Communication Engineers.